A feasible study on the model predictive control for docking approach of small spacecraft using thrusters and a control moment gyro

Katsuyoshi Tsujita

Abstract— This paper deals with maneuver control for the autonomous docking of two small spacecraft in a rendezvous flight. Due to hardware constraints, maneuver control suppressing fuel consumption and computational cost is a significant issue for small spacecraft. Here, the maneuver control for the approaching motion used a model predictive control system. The spacecraft's maneuvers in two-dimensional plane motion were performed in a frictionless environment with air bearings to verify the control performance.

I. INTRODUCTION

With the rapid increase in the number of small spacecraft utilization missions in space engineering in recent years, the establishment of motion control technology using multiple small spacecraft has been widely studied[1]-[7]. In such a trend, autonomous docking technology from rendezvous flight of numerous small spacecraft is one key technology. This paper considers two small spacecraft and deals with the maneuver control for autonomous docking that realizes the approach from their rendezvous flight to just before the execution of docking between the spacecraft. One of the difficulties of autonomous docking technology for small spacecraft is that the hardware constraints are more severe than those for large spacecraft. For example, it is difficult for small spacecraft to be equipped with many propulsion thrusters, sufficient power supply, and high-precision relative position sensors. Also, the processing capacity of the control computer is lower than that of large spacecraft. Therefore, a small spacecraft's autonomous docking maneuver control system must be designed within the optimal control framework[8]-[13].

This study considers two small spacecraft in rendezvous flight status in Earth orbit. Then, a maneuver to autonomously approach one of them from the rendezvous state to the position just before docking with the other spacecraft is realized using model predictive control (MPC). We designed the spacecraft's motion control system while predicting the control inputs that minimize the energy consumption of the system's attitude control actuators and fuel consumption for propulsion. The small spacecraft handled in this study is assumed to be a microcomputer with low computational power. Furthermore, the spacecraft should have propulsion thrusters and a very small CMG (Control Moment Gyro) for attitude control torque generated by the gimbal mechanism that supports the rotation axis of the flywheel[14].

Katsuyoshi Tsujita are with Dept. of Mechanical and Aerospace Engineering, Tottori University, Tottori 680-8550, Japan
ktsujita@tottori-u.ac.jp

According to recent studies on the control design of mechanical systems, model predictive control has been formulated in the framework of optimal control, and its effectiveness has been confirmed in various actual machines[15]. A cost function is first set in the optimal control framework, and the control input that minimizes it is obtained. The optimal control problem is to numerically solve a two-point boundary value problem under these conditions, given the starting and ending points of the state variables. In general, offline solving involves a huge amount of iterative computations. In addition, the control inputs obtained are open-loop control, which is sensitive to model errors and disturbances. In contrast, model predictive control is a robust algorithm that sets a specific prediction time, solves the optimization problem within this prediction time, and obtains the control input in real time. It is characterized by its ability to compensate for model errors and disturbances and its feedback control structure.

On the other hand, according to space agencies in various countries, ground tests using hardware models and numerical simulations are mandatory during the development phase of spacecraft and basic research to evaluate spacecraft performance and verify mission feasibility to achieve a given space mission. Therefore, it is significant that this study confirmed the feasibility of maneuver control in the framework of optimal control of a small spacecraft with limited hardware resources in an experimental ground test using an actual hardware model.

This study aimed to fabricate a mock-up of small spacecraft hardware close to the actual machine and obtain primary data to evaluate the effectiveness and performance of the maneuver control system designed in the framework of the optimal control of small spacecraft through ground experiments. Hardware experiments of the maneuver control of a small spacecraft were conducted using the designed model predictive control system. Since the hardware experiments were under Earth's gravity, the author conducted maneuver control experiments on a two-dimensional plane using air bearings in a micro-friction environment[16][17]. The small mock-up spacecraft was about 30 cm cubic and equipped with four small air jet thrusters and a single-axis CMG. The target spacecraft's docking port and relative position can be measured using a small onboard camera. Model predictive control reduces the propellant consumption of the thrusters and the drive energy consumption of the CMGs, allowing an autonomous approach to the target docking port with sufficient accuracy.

II. Model

The geometric relationship between a small spacecraft and the docking port on the other side to which it will dock is shown in Figure 1. Assume that the target docking port is at the origin of the world coordinate system. Initially, two spacecraft are assumed to be in a rendezvous flight and separated by a certain distance. Then, we consider the problem of controlling the position and attitude of one spacecraft to bring it closer to the vicinity of the target port location.
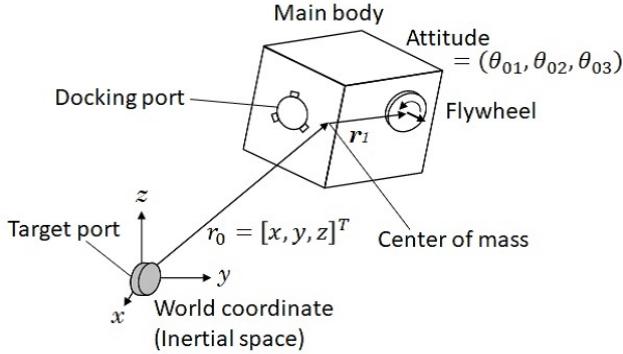

Fig. 1. Schematic model of the chaser spacecraft and docking target.

The following vectors are defined.
- $r_0 = [x, \ y, \ z]^T$: the position of the main body's center of mass from the world coordinate origin.
- $\theta_0 = [\theta_{01}, \ \theta_{02}, \ \theta_{03}]^T$: Euler angle expressing the attitude of the spacecraft to the world coordinate.

The state variable for equations of motion is defined as follows:

$$Z = [\dot{r}_0^T, \ \omega_{10}^T]^T \qquad (1)$$

where ω_{10} is the angular velocity vector of the main body.

We defined the input force/torque vector u corresponding to the state variable Z as follows:

$$u = [F_{th}^T, \ \tau_G^T]^T \qquad (2)$$

The equation of motion of the spacecraft is described as follows:

$$M\dot{Z} + h = Bu \qquad (3)$$

where M, h and B are mass matrix, nonlinear term and input coefficient matrix, respectively.

$F_{th} = [F_x, F_y, F_z]^T$ and $\tau_G = [\tau_{G1}, \tau_{G2}, \tau_{G3}]^T$ are the thruster's input force vector and the input torque of the CMG Gimbal mechanism. The input torque of the CMG generates the gyro moment of the flywheel, and it moves the attitude motion of the main body.

The angular velocity vector and the time derivative of the Euler angle have the following relation.

$$\omega_{10} = S_{10}(\theta_{01}, \ \theta_{02} \ \theta_{03}) \begin{bmatrix} \dot{\theta}_{01} \\ \dot{\theta}_{02} \\ \dot{\theta}_{03} \end{bmatrix} \qquad (4)$$

where matrix $S_{10}(\theta_{01}, \ \theta_{02} \ \theta_{03})$ is the function of Euler angles.

III. Model predictive control

A. Formulation

This study assumed that the spacecraft has CMG for attitude control and chemical thrusters for position control. However, a small spacecraft has little energy and fuel resources. Therefore, we designed the optimal controller to reduce the actuator power and thruster's fuel consumption.

State variable $X \in \mathbb{R}^{12}$ for the controller is defined using the position and Euler angle of the main body as follows:

$$X = \begin{bmatrix} \dot{r}_0^T, & \omega_{10}^T, & r_0^T, & \theta_0^T \end{bmatrix}^T \qquad (5)$$

We designed a model predictive control (MPC) system as follows. First, we introduce an auxiliary variable, s, related to time, and the model prediction time (the horizon) as T. Then, at the moment of t, $s = 0$, and the end time of s is set to $s = T$. Using this auxiliary variable s, let the cost function be the evaluation function in the interval $[0, T]$ concerning s as follows:

$$\mathscr{J} = \psi(X(t+T)) + \int_0^T L(u)ds \qquad (6)$$

We formulated the cost $L(u)$ as the thruster's fuel consumption and CMG's electrical energy consumption. It should be noted here that the cost function $L(u)$ is a function of the control input u only and not the state variable X. This is because, in this study, the spacecraft is in a rendezvous state in Earth's orbit. Therefore, there are no restrictions on the path to docking, so there is no need to include the state variable in the cost function.

$X(t+T)$ is the state variable at the end time of the model predictive horizon T. The controller only has to approach the spacecraft close enough. After the approach maneuver, the succeeding docking procedure will be implemented. The objective of the approach maneuver in this study is not to reach the docking port strictly. Therefore, this study introduced the constraints on the state variables at the end time of the horizon using a quadratic form in the cost function.

$\psi(X(t+T))$ is formulated as the quadratic form with weight parameter P. On the other hand, the thruster's fuel consumption and the CMG's energy consumption are evaluated by the cost function $L(u)$.

$L(u)$ and $\psi(X(T))$ are defined as follows:

$$L(u) \quad = \quad u^T Q u \qquad (7)$$

$$\psi(X(t+T)) \quad = \quad X^T(t+T)PX(t+T) \qquad (8)$$

where $Q \in \mathbb{R}^{6 \times 6}$ and $P \in \mathbb{R}^{12 \times 12}$ are positive definite matrices.

By using the Lagrangian multiplier $\lambda \in \mathbb{R}^{12}$, Hamiltonian is defined as follows:

$$H(X, u, \lambda, t) = L(u) + \lambda^T f(X, u, t) \qquad (9)$$

where $f(X, u, s)$ is denoted from Eq. (3) as follows:

$$f(X, \ u, \ s) = \begin{bmatrix} M^{-1}(Bu - h) \\ \dot{r}_0 \\ S_{10}^{-1}\omega_{10} \end{bmatrix} \qquad (10)$$

The constraint condition is derived as follows:

$$\left(\frac{\partial H}{\partial u}\right)^T (X,u,\lambda,t) = 0 \tag{11}$$

Let time t be the initial time and time $t+T$ be the final time. This time interval is divided into N. Then Δt is the sampling time and $T + k\Delta t, (k = 0,1,\cdots,N-1)$ is the optimal control input $\hat{u}_k(t)$ at discrete time $t + k\delta t, (k = 0,1,\cdots,N-1)$. The state variable and Lagrangian multiplier when the system receives the input $\hat{X}_k(t)$ and $\hat{\lambda}_k(t)$, respectively.

The vector $U(t)$ summarizing the discrete control inputs is defined as follows.

$$U(t) = \begin{bmatrix} \hat{u}_0(t) \\ \hat{u}_1(t) \\ \vdots \\ \hat{u}_{N-1}(t) \end{bmatrix} \tag{12}$$

For the vector $U(t)$, Eq.(11) becomes the following algebraic equation.

$$F = \begin{bmatrix} \left(\frac{\partial H}{\partial u}\right)^T (\hat{X}_0(t),\hat{u}_0(t),\hat{\lambda}_0(t),t) \\ \vdots \\ \left(\frac{\partial H}{\partial u}\right)^T (\hat{X}_{N-1}(t),\hat{u}_{N-1}(t),\hat{\lambda}_{N-1}(t),t+T) \end{bmatrix} = O \tag{13}$$

We can find an unknown vector $U(t)$ that satisfies Eq.(13), but we need to reduce the amount of computation for this purpose. Therefore, we consider a differential equation for F and a mechanism to converge to zero with a time constant of $1/\zeta$ (>0).

$$\frac{\partial F}{\partial U}\dot{U}(t) = -\zeta F - \frac{\partial F}{\partial X}\dot{X}(t) - \frac{\partial F}{\partial t} \tag{14}$$

By viewing Eq.(14) as an algebraic equation for $\dot{U}(t)$ and obtaining $\dot{U}(t)$ numerically, and integrating $\dot{U}(t)$ we can obtain the discrete-time control input $U(t)$. In this study, we utilized the Generalized Minimal Residual method (GMRES) to solve Eq.(14) algebraically. The GMRES method is an approximate solution algorithm that can solve simultaneous linear equations quickly and is commonly used in MPC. Therefore, we also used this method in this study.

In order to compare the performance with the model predictive control system, a simple PD feedback control system was designed with low computational cost. First, define V as a candidate Lyapunov function with the state variable $Y = [\,x,\ y,\ \theta_{03}\,]^T$ as follows:

$$V = \frac{1}{2}Y^T K_P Y + \frac{1}{2}\dot{Y}^T\dot{Y} \tag{15}$$

Differentiate Eq.(15) with time along the equation of motion, and equate it with $-K_D\dot{Y}$ to be negative definite. K_D is the feedback gain for damping. We can obtain the control input u_L as follows:

$$u_L = -B^{-1}M\left(K_P Y + K_D\dot{Y}\right) + B^{-1}h \tag{16}$$

The feedback gains K_P, K_D were determined by trial and error so that the ideal convergence time constant from the initial values of position and angle in the model predictive control would be approximately the same as the ideal convergence time constant.

IV. Hardware experiments

To verify the performance and validity of the controller, we implemented hardware experiments in a two-dimensional environment.

A. Hardware specifications

The specification of the spacecraft and experimental environment are summarized in Table I. The target ddocking port is located and fixed at the world coordinate's origin. With air bearings, the friction between the mockup spacecraft and the experimental field is so tiny as to be negligible.

TABLE I
SPECIFICATION OF THE EXPERIMENTAL SETUP.

Mockup spacecraft	
Size W × D × H	0.30 m × 0.30 × 0.30 m
Total weight	4.5 kg
Air bearings	New way air bearings,
	Inc. S104001 × 3 at 0.40 MPa
Thrusters	Air thrust × 4 Thrust: 1.2 N
Attitude actuator	1-axis CMG (Flywheel: 3000 rpm)
On-board processor	
Controller	Cortex-A72 1.5 GHz 8GB Main memory
Camera	3280 px × 2464 px
Experimental field	
Test field W × D	1.5 m × 0.9 m

Figure 2 shows the structure of a mockup model of the small spacecraft for a hardware experiment. The mockup has a microcomputer as a control unit and an onboard camera to recognize the docking target. In addition, the spacecraft is equipped with four thrusters as actuators for spacecraft motion and a small CMG with one axis for attitude control.
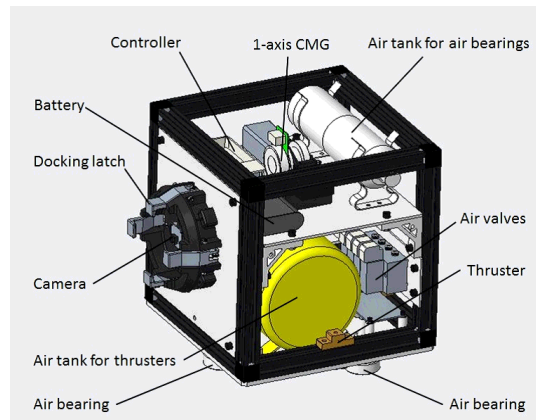

Fig. 2. The design of the mockup spacecraft.

Figure 3 shows the architecture of the hardware system. The central controller onboard is a microcomputer with

Quad-core Cortex-A72 1.5GHz. The microcomputer controls the thruster valves and CMG. In addition, a CMOS camera is equipped in the center of the spacecraft's docking port to detect the target port.

The center of the target port is equipped with an ArUco marker[18]. The relative position and the spacecraft's attitude to the target port are computed using real-time image data of the ArUco marker, which is available in the OpenCV software library.
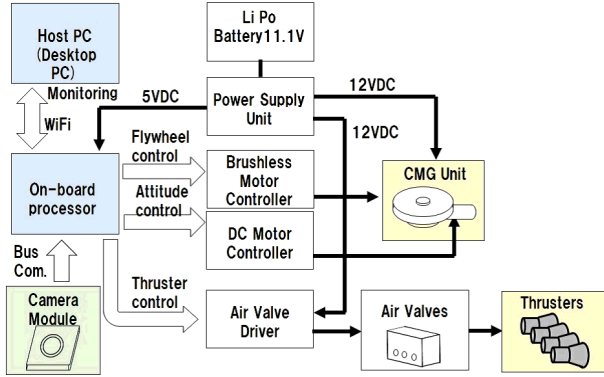

Fig. 3. Mockup spacecraft system architecture for hardware experiment.

B. Actuators

The output of the thruster in the hardware experiment is a binary On/Off control. Propulsion was realized from the control inputs obtained by the model predictive control system calculations by opening and closing the fuel valves of the actual hardware thruster.

$$
F_i = \begin{cases} F_{ON} & : \hat{u}_i, > \varepsilon \\ 0 & : -\varepsilon < \hat{u}_i < \varepsilon \qquad i = x, \ y \\ -F_{ON} & : \hat{u}_i < -\varepsilon \end{cases} \qquad (17)
$$

In the hardware experiments, $\varepsilon = 0.01$N was used. Although this value is arbitrary, it considers that in preliminary experiments, the spacecraft in the experimental setup hardly moved at thrusts below this level due to the very slight friction of the air bearings. F_{ON} is the thruster output when the valve for the thruster gas is turned on. The gas ejection dynamics is complex and not constant, but the maximum measured value was about 1.2 N.

C. Measurement of spacecraft's relative position

The onboard camera we used to detect the spacecraft's relative position and angle of the target port has image distortion. We identified the camera parameters and corrected the image distortion using Zhang's method [19]. The algorithm is a well-known method to estimate and calibrate the camera's position and the optical axis using a flat plane image such as a chessboard image pattern. A 2D (2-dimensional) point on the camera coordinate is denoted by $m = [u, v]^T$. A 3D point in the world coordinate is denoted by $M = [X, Y, Z]^T$. A camera's image projection model is expressed as follows:

$$
s\tilde{m} = B[R \ t]\tilde{M} \qquad (18)
$$

where $\tilde{m} = [m^T, 1]^T \in \mathbb{R}^3$ and $\tilde{M} = [M^T, 1]^T \in \mathbb{R}^4$ are the augmented vectors. Parameter s is an arbitrary scale factor that expresses the camera's image distortion. R, t are the rotation matrix and translation vector which transform the world coordinate system to the camera coordinate system. Matrix B is the camera's intrinsic matrix that involves parameters of the focal length and the optical center position of the camera. We identified the parameters s and B, and compensated for the image distortion. The image position-estimation error obtained from the calibrated image was about 2.4E-03 m at maximum.

In this study, the relative position of the spacecraft to the target port is calculated by using image data. The center of the target port is equipped an ARUCO marker. The position of the space craft is measured using the ARUCO marker which is available in OpenCV software library. Figure 4 shows the AR marker equipped on the center of target port in this study.
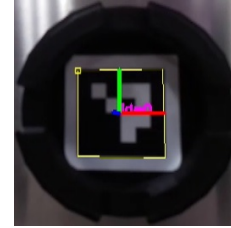

Fig. 4. Captured image of the onboard camera of the spacecraft. On the target port's center, an AR marker is equipped for the spacecraft to identify the target.

D. Experimental field

Figure 5 shows a snapshot of the experimental hardware setup. The mockup spacecraft hovers on the experimental field with air bearings by 6 μm gap. The mockup spacecraft has air tanks to supply the air to the air bearings and thrusters. The capacity of the air tank is 2.7×10^{-3} m^3. The system has its battery and control devices and autonomously controls its motion onboard. The host computer monitors the system and gets real-time images captured by the onboard camera. In this study, the target and docking ports have no controlled device to dock or latch mechanism. Therefore, the final approach point for the spacecraft is the target port.
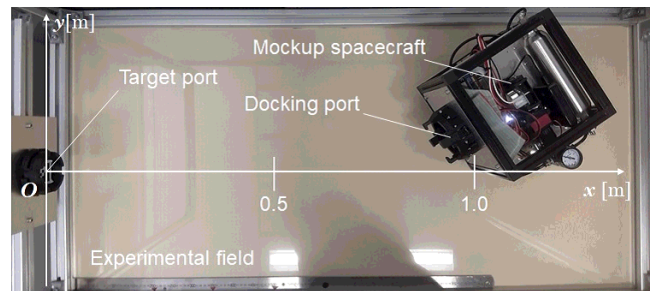

Fig. 5. Experimental setup. The mockup spacecraft is floating on the surface plate with air bearings. The target port is fixed on the frame structure of the experimental field.

E. Setting parameters

Weight parameters for the model predictive control are determined to evaluate the thrusters' output and energy consumption of the CMG. The components of the matrix Q mean the weight parameter of the thrusters' forces $(1.0, 1.0)$ and the coefficient of Joule's energy consumption of the CMG's motor (0.82).

$$P = diag[10.0, 10.0, 10.0, 10.0, 10.0, 10.0] \quad (19)$$
$$Q = diag[1.0, 1.0, 0.82] \quad (20)$$

Feedback gains of the simple PD feedback control for performance comparison are set as follows:

$$K_P = diag[0.0775, 0.1], \quad K_D = diag[0.4, 0.6] \quad (21)$$

V. EXPERIMENTAL RESULTS

Figures 6 and 7 show the results of hardware experiments with maneuver control from various initial positions to the target. Figure 7 is a projection of Fig.6 onto the x-y plane. In Figure 7, the initial attitude angle of the spacecraft is not represented. The circles and triangles in the figure indicate successful and unsuccessful initial positions, respectively. Success was judged based on whether the distance between the target port and the spacecraft docking port was closer than 0.05 m during the specified control time (10.0 sec). The reason for setting the judgment distance to 0.05 m is that the distance can be considered a distance at which soft docking by electromagnets is possible in the second stage of the docking mission.

As can be seen from the figure, if the initial position of the spacecraft is more than about 0.5 m from the target port, the maneuver succeeds in most cases. Conversely, the maneuver almost always fails if the spacecraft's initial position is within about 0.5 m. These results are due to the initial position being too close to the target. This system is a fully actuated, with equal degrees of freedom of the actuators relative to the degrees of freedom available for movement. However, in the control system design, the thruster is modeled as an actuator capable of continuous output, but in reality, it is an actuator with only binary ON/OFF control. Therefore, if the initial position is too close to the target, it cannot output even if the control system requires a weak continuous output. Furthermore, as position and attitude errors accumulate, the maximum output is suddenly generated, making positioning difficult. Therefore, when performing model predictive control using an actuator with such discontinuous outputs, a formulation that considers discontinuities in the actuator model is needed in the future.

Figures 8 and 9 show the position and angular error of the spacecraft's docking port relative to the target at the end time in the hardware experiment. In the experiment, the position and angle errors at the end time are compared between the case with the model predictive control system and the case with the feedback control system. In both cases, it is clear that MPC performs better with limited hardware resources.

Figure 10 compares the thrusters' fuel consumption and the CMG's electrical energy consumption for each control
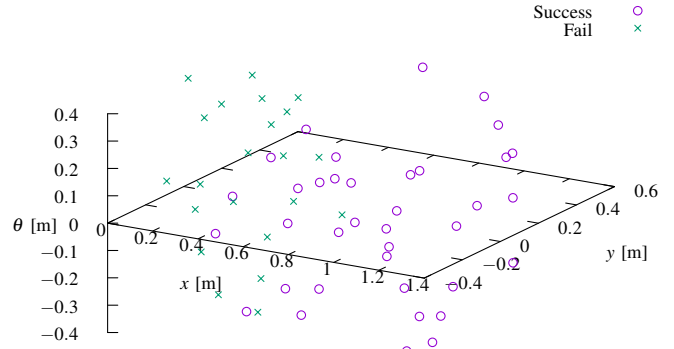

Fig. 6. The results of hardware experiments with maneuver control from various initial positions to the target (N=50 trials).
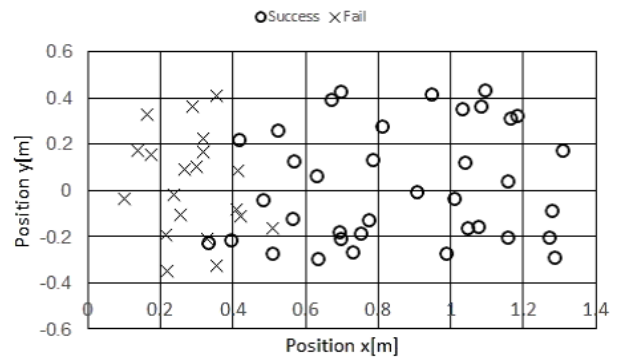

Fig. 7. The results of hardware experiments with maneuver control from various initial positions to the target (N=50 trials).
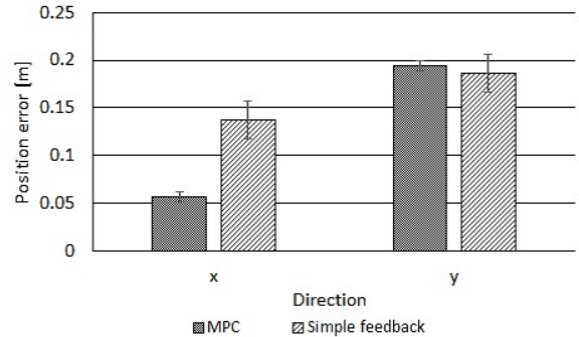

Fig. 8. Position error of the docking port against the target (N=50 trials).

law. Both results are summarized from 50 hardware experiments. Figure 10 (a) shows that the thruster fuel consumption is more suppressed with the model predictive control than with the simple feedback control. On the other hand, Figure 10 (b) shows that the energy consumption of the CMG is suppressed less by the feedback control law. In this hardware experiment, the model predictive control law is weighted to the thruster fuel consumption due to the small capacity of the thruster fuel tanks. Therefore, in Figure 10 (b), the energy consumption of the CMG for attitude control is used more.
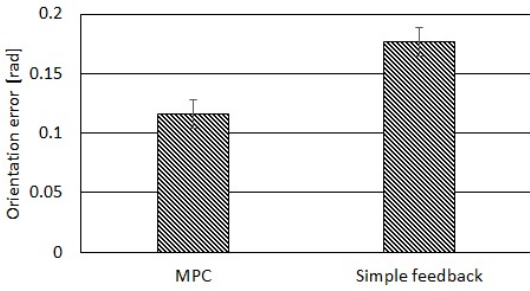
Fig. 9.   Orientation error of the docking port against the target (N=50 trials).

(a) Thrusters' fuel consumption
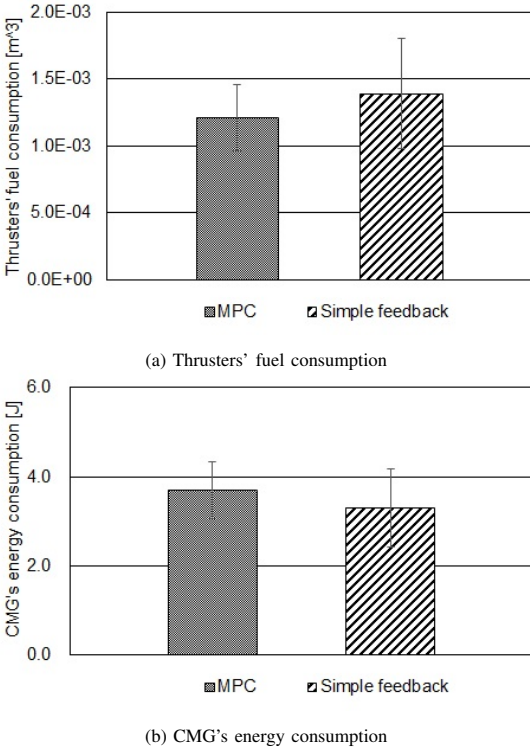

(b) CMG's energy consumption

Fig. 10.   Comparison of thrusters' fuel consumption CMG's energy consumption in each control method.

VI. Conclusions

The performance and feasibility of maneuver control using the model predictive control law for autonomous docking of small spacecraft was verified through hardware experiments using a spacecraft mockup. For the model predictive controller design, the cost function was constructed from the norm of the control input and the position error. Hardware experiments validated the effectiveness of the approach maneuver just prior to docking within the allowable maneuvering error in a realistic situation. Furthermore, we verified the approach maneuver to be sufficiently accurate over a wide approach area and to reduce thruster fuel consumption using the proposed controller.

Due to the small capacity of the thruster fuel tanks in the hardware experiments, the model predictive controller

in this paper focuses heavily on thruster fuel consumption. Therefore, more energy is consumed by the CMG for attitude control. This performance is strongly dependent on hardware specifications and resources. Therefore, we have the design freedom to choose the weight coefficients of the cost function in the model predictive control according to the mission and hardware specifications.

The computational cost of the model predictive controller designed in this study is higher or comparable to simple feedback control. Therefore, the next step in this study is a plan to reduce the computational cost of the controller.

References

[1] Jing Pei, et al., Autonomous Rendezvous and Docking of Two 3U Cubesats Using a Novel Permanent-Magnet Docking Mechanism, 54th AIAA Aerospace Sciences Meeting, 10.2514/6.2016-1465, 2016.

[2] D.Wang, B.Wu, and E.K.Poh, Satellite Formation Flying, Springer Science+Buisiness Media Singapore, 2017.

[3] D.J. Barnhart, T.Vladimirova, and M.N.Sweeting, Very-Small-Satellite Design for Distributed Space Missions, Journal of Spacecraft and Rockets, Vol. 44, No. 6, pp.1294-1306, 2007.

[4] S. Eckersley, et al., In-Orbit Assembly of Large Spacecraft Using Small Spacecraft and Innovative Technologies, Proceedings of the 69th International Astronautical Congress (IAC),IAC-18,B4,6A,1,x43225, 2018.

[5] Rebecca C. Fousta et al., Ultra-Soft Electromagnetic Docking with Applications to In-Orbit Assembly, Proc. of the 69th International Astronautical Congress (IAC), IAC-18-C1.6.3, 2018.

[6] Reiter, J, Terry, M, B ̈ohringer, KF, Suh, JW, and Kovacs, GTA., Thermo-Bimorph Microcilia Arrays for Small Spacecraft Docking, Proceedings of the ASME 2000 International Mechanical Engineering Congress and Exposition, pp. 57-63, 2000.

[7] L.Olivieri, A.Francesconi, Design and test of a semiandrogynous docking mechanism for small satellites, Acta Astronautica, Vol.122, pp/219-230, 2016.

[8] I.M.Ross, M.Karpenko, A review of pseudospectral optimal control: From theory to flight, Annual Reviews in Control, 36(2), pp.182-197, 2012.

[9] B.Senses and A.V.Rao, Optimal Finite-Thrust Small Spacecraft Aeroassisted Orbital Transfer, Journal of Guidance, Control, and Dynamics, Vol. 36, No. 6, pp.1802-1809, 2013.

[10] Ming, Xin, Hejia Pan, Indirect Robust Control of Spacecraft via Optimal Control Solution, IEEE Transactions on Aerospace and Electronic Systems, 48(2), pp.1798-1809, 2012.

[11] H.Shen and P.Tsiotras, Time-Optimal Control of Axisymmetric Rigid Spacecraft Using Two Controls, Journal of Guidance, Control, and Dynamics, Vol. 22, No. 5, pp.682-694, 1999.

[12] Yongqiang Qi, Yingmin Jia, Constant thrust fuel-optimal control for spacecraft rendezvous, Advances in Space Research, 49(7), pp.1140-1150, 2012.

[13] J.B.Thevent, R.Epenoy, Minimum-Fuel Deployment for Spacecraft Formations via Optimal Control, Journal of Guidance, Control, and Dynamics, Vol.31, No.1, pp.101-113 ,2008.

[14] K.Omagari, K.Fujihashi, S.Matunaga, CMG Configuration and Control for Rapid Attitude Maneuver of Small Spacecraft, 9th International Symposium on Artificial Intelligence, Robotics and Automation in Space, 2008.

[15] JAXA, Engineering Requirement, Guideline, https://sma.jaxa.jp/en/TechDoc/index.html

[16] Y.K.Nakka, et al., Six degree-of-freedom space-craft dynamics simulator for formation control research, 2018 AAS/AIAA Astrodynamics Specialist Conference, 2018.

[17] J.L.Schwartz, M.A.Peck, C.D.Hall, Historical Review of Air-Bearing Spacecraft Simulators, Journal of Guidance, Control, and Dynamics, Vol.26, No.4, 2003.

[18] Detection of ArUco Markers, https://docs.opencv.org/4.5.2/d5/dae/tutorial_aruco_detection.html

[19] Zhang, Z.: A Flexible New Technique for Camera Calibration, IEEE Transactions on Pattern Analysis and Machine Intelligence, 22(11) (2000), 1330-133.